© 2020. Published by The Company of Biologists Ltd | Development (2020) 147, dev186593. doi:10.1242/dev.186593

RESEARCH REPORT

Lgl cortical dynamics are independent of binding to the Scrib-Dlg complex but require Dlg-dependent restriction of aPKC

Guilherme Ventura*,‡, Sofia Moreira‡, André Barros-Carvalho, Mariana Osswald and Eurico Morais-de-Sá§

ABSTRACT

Apical-basal polarity underpins the formation of epithelial barriers that are crucial for metazoan physiology. Although apical-basal polarity is long known to require the basolateral determinants Lethal Giant Larvae (Lgl), Discs Large (Dlg) and Scribble (Scrib), mechanistic understanding of their function is limited. Lgl plays a role as an aPKC inhibitor, but it remains unclear whether Lgl also forms complexes with Dlg or Scrib. Using fluorescence recovery after photobleaching, we show that Lgl does not form immobile complexes at the lateral domain of *Drosophila* follicle cells. Optogenetic depletion of plasma membrane PIP_2 or *dlg* mutants accelerate Lgl cortical dynamics. However, Dlg and Scrib are required only for Lgl localization and dynamic behavior in the presence of aPKC function. Furthermore, light-induced oligomerization of basolateral proteins indicates that Lgl is not part of the Scrib-Dlg complex in the follicular epithelium. Thus, Scrib and Dlg are necessary to repress aPKC activity in the lateral domain but do not provide cortical binding sites for Lgl. Our work therefore highlights that Lgl does not act in a complex but in parallel with Scrib-Dlg to antagonize apical determinants.

KEY WORDS: Epithelial cell, Apical-basal polarity, Basolateral determinants, FRAP, *Drosophila*, Lgl, Dlg

INTRODUCTION

Cell polarity is a fundamental property that enables epithelia to act as selective barriers between different environments. Epithelial architecture relies on the asymmetric segregation of evolutionary conserved polarity proteins that define the apical and lateral domains, and correctly position intercellular junctions (Flores-Benitez and Knust, 2016). Lgl is one such regulator of apical-basal polarization (Bilder et al., 2000) that is also necessary for polarization in a range of different contexts, including stem cell division (Ohshiro et al., 2000; Peng et al., 2000), front-rear polarization (Dahan et al., 2014), and anterior-posterior polarization of *Drosophila* oocytes (Fichelson et al., 2010; Tian and Deng, 2008) and *C. elegans* embryos (Beatty et al., 2010; Hoege et al., 2010).

Lgl localizes below the adherens junction to promote basolateral identity together with Scrib and Dlg. These genes were originally described in *Drosophila*, where homozygous mutants display epithelial disorganization and neoplastic growth (Bilder et al., 2000; Gateff, 1978; Woods and Bryant, 1989). Further analysis placed these genes in a basolateral polarity module due to their mutually interdependent localization and antagonistic genetic interactions with the apical Crumbs and aPKC complexes (Bilder et al., 2003; Tanentzapf and Tepass, 2003). Although Scrib, Lgl and Dlg accumulate exclusively at the occluding septate junction in the adult *Drosophila* midgut, where they are dispensable for apical-basal polarity (Chen et al., 2018), their cortical localization plays evolutionarily conserved roles in polarity and adhesion (Chalmers et al., 2005; Dow et al., 2003; Grifoni et al., 2007; Legouis et al., 2003; McMahon et al., 2001; Müsch et al., 2002; Raman et al., 2016; Russ et al., 2012; Sripathy et al., 2011; Yamanaka et al., 2006). Loss-of-function phenotypes are, however, masked in mammalian epithelia by the presence of multiple paralogues, or, in the case of Scrib, by the compensatory function of proteins with a similar leucine-rich repeat and PDZ protein (LAP) domain (Choi et al., 2019).

The molecular basis for the function of basolateral proteins is still unclear. The predominant hypothesis is that Scrib and Dlg ensure Lgl localization at the lateral cortex (Bilder et al., 2000; Kallay et al., 2006; Zeitler et al., 2004). In turn, Lgl prevents the extension of apical determinants (Hutterer et al., 2004), likely by inhibiting the aPKC-Par-6 complex (Atwood and Prehoda, 2009; Betschinger et al., 2003; Yamanaka et al., 2003, 2006), and promoting Crumbs recycling from the lateral cortex (Fletcher et al., 2012). X-ray crystallography revealed an interaction between mammalian Lgl2 and the guanylate kinase domain of Dlg4 (Zhu et al., 2014). Moreover, Lgl may bind to the LAP unique region of Scrib (Kallay et al., 2006), in particular to a small region termed LAPSDa (Choi et al., 2019). Nevertheless, it remains unknown whether Scrib and Dlg bind Lgl *in vivo* to control its function and localization in the lateral domain. Dlg and Scrib are also likely to play roles independently of Lgl. Recent studies uncovered specific phenotypes for *dlg* and *scrib* mutants on adherens junction and tricellular junction formation in *Drosophila* embryonic and wing disk epithelia, respectively (Bonello et al., 2019; Sharifkhodaei et al., 2019). Furthermore, whereas Scrib and Dlg cooperate to orient the mitotic spindle (Bergstralh et al., 2013; Nakajima et al., 2013, 2019), Lgl release from the cortex promotes planar spindle orientation (Bell et al., 2015; Carvalho et al., 2015).

Lgl cortical localization is inhibited by phosphorylation, which is controlled by aPKC, Aurora A and Protein Phosphatase 1 (Bell et al., 2015; Betschinger et al., 2003; Carvalho et al., 2015; Moreira et al., 2019). Early studies highlighted the association of Lgl with the actomyosin cytoskeleton (Betschinger et al., 2005; Strand et al., 1994), whereas recent work uncovered that Lgl cortical localization is mediated by interactions between its basic and hydrophobic domain and membrane phosphoinositides, primarily phosphatidylinositol-4,5-biphosphate (PIP_2) (Bailey and Prehoda, 2015; Dong et al., 2015; Visco et al., 2016). These binding partners could aid Scrib and Dlg in forming multivalent interactions that regulate Lgl binding at the lateral cortex, but the contribution of each putative interactor has not been

i3S (Instituto de Investigação e Inovação em Saúde, Universidade do Porto) and IBMC (Instituto de Biologia Molecular e Celular), Rua Alfredo Allen, 208, 4200-135 Porto, Portugal.
*Present address: Novo Nordisk Foundation Center for Stem Cell Biology (DanStem), University of Copenhagen, Copenhagen, Denmark.
‡These authors contributed equally to this work

§Author for correspondence (eurico.sa@ibmc.up.pt)

E.M.-d.S., 0000-0003-3525-8231

Handling Editor: Thomas Lecuit
Received 10 December 2019; Accepted 2 July 2020

Development (2020) 147, dev186593. doi:10.1242/dev.186593

defined. Here, we have characterized the mechanisms that regulate Lgl cortical dynamics in the *Drosophila* follicular epithelium. Lgl dynamics are dependent on both PIP_2 and Dlg. However, whereas PIP_2 restricts Lgl cortical mobility, Dlg and Scrib regulate Lgl by repressing aPKC ectopic localization. Moreover, we detect the presence of Dlg-Scrib complexes that do not contain Lgl, reinforcing that Lgl antagonizes apical proteins independently of Scrib and Dlg.

RESULTS AND DISCUSSION

Lgl displays membrane-diffusion behavior and faster dynamics than Dlg and Scrib

To characterize Lgl dynamics in the lateral domain of epithelial cells, we performed fluorescence recovery after photobleaching (FRAP) in post-mitotic stages 7 to 9 of the *Drosophila* follicular epithelium (Fig. S1). We first compared the cortical dynamics of Lgl with Scrib and Dlg using GFP-tagged proteins expressed at endogenous levels. Lgl is significantly more dynamic than Dlg and Scrib ($Lgl^{t1/2}$ ~10 s; $Dlg^{t1/2}$ ~40 s; $Scrib^{t1/2}$ ~60 s; Fig. 1A,B, Movie 1), likely reflecting their distinct binding domains and individual functions (Bonello and Peifer, 2019; Stephens et al., 2018). Moreover, rebleaching a previously bleached region leads to an identical plateau of Lgl fluorescence recovery (Fig. 1C). Thus, Lgl does not form a significant subpopulation of immobile complexes at the cortex and plasma membrane.

FRAP kymographs show that fluorescence recovery initiates at the edges of the photobleached region (Fig. 1B, arrow), suggesting that Lgl diffuses laterally along the membrane. Consistent with this, fluorescence decreases in neighboring membranes immediately after bleaching (Fig. 1D). Similar behavior is observed for the GFP tagged pleckstrin homology (PH) domain of Phospholipase Cδ, which binds $PI(4,5)P_2$ (Fig. S2A,B). These results emphasize the contribution of membrane diffusion to Lgl mobility, but do not exclude the significance of membrane-cytoplasm exchange. In fact, both types of mobility contribute for the dynamic behavior of proteins that bind PIP2 (Goehring et al., 2010; Hammond et al., 2009). Fluorescence recovery via diffusion scales with the size of the photobleached region (Fritzsche and Charras, 2015; Sprague and McNally, 2005). Thus, we reduced the size of the photobleached region to verify whether bi-exponential fitting could separate the contribution of membrane diffusion. However, the reduced distance that unbleached molecules must diffuse decreases both $t^{1/2fast}$ and $t^{1/2slow}$, indicating that membrane diffusion contributes for both half-times (Fig. 1E). Therefore, we subsequently compared the mobility of Lgl under different experimental conditions through a single half-time of fluorescence recovery (Table S1, see Materials and Methods).

Lgl dynamics in the lateral domain are restrained by PIP_2 and independent of aPKC

Interactions between Lgl and putative binding partners should restrict Lgl mobility in the lateral cortex. We used FRAP to determine the relative contributions of known Lgl interactors, PIP_2 and the actin cortex. Lgl remains in the cortex after disruption of the actin cytoskeleton with Latrunculin A (LatA) in the embryonic epithelium (Dong et al., 2015). LatA also does not affect the localization of either Lgl, Dlg or Scrib, suggesting that follicle cells remain polarized upon acute actin cytoskeleton disruption (Fig. 2A, Fig. S3). However, LatA induced a minor but significant acceleration of Lgl-GFP fluorescence recovery (Fig. 2B). This does not result from pleotropic effects on membrane dynamics as PH-GFP fluorescence recovery is unchanged by LatA (Fig. S2C).

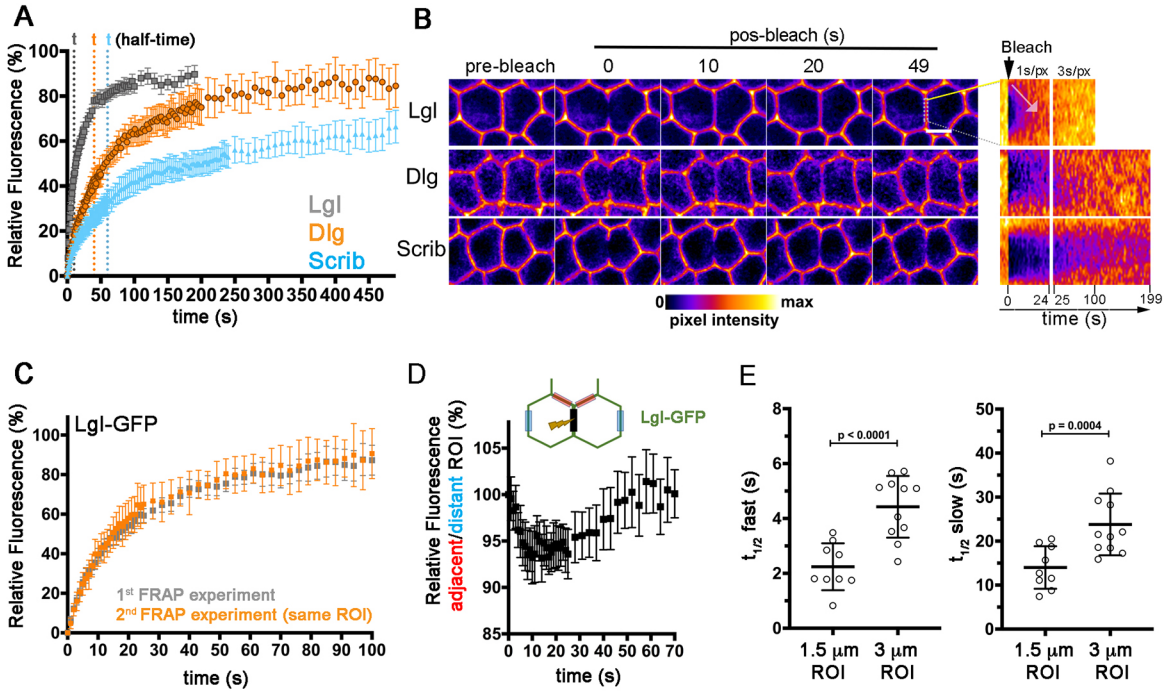

Fig. 1. Lgl cortical dynamics are faster than Scrib and Dlg, and are coupled to membrane-diffusion. (A) Fluorescence recovery (±95% CI) of endogenously tagged Lgl-GFP (n=43), Dlg-GFP (n=18) and Scrib-GFP (n=22). (B) Pseudo-colored images of FRAP in the lateral domain of the follicular epithelium (Movie 1). Kymographs depict fluorescent recovery in the photobleached region. Scale bar: 5 µm. (C) Recovery plots of consecutive FRAP experiments in the same ROI (n=11). (D) Lgl-GFP mean intensity (±95% CI, n=23) in the interface adjacent (red) to the bleached region normalized to the mean intensity of distant interfaces (blue). (E) Half-times ($t_{1/2}$; ±s.d.) for the fast and slow components of Lgl-GFP dynamics were obtained with a bi-exponential fit of recovery curves for varying photobleaching size [1.5 µm (n=9), 3 µm (n=11)]. Data are mean±s.d. P-values calculated with a Mann–Whitney U-test.

Development (2020) 147, dev186593. doi:10.1242/dev.186593

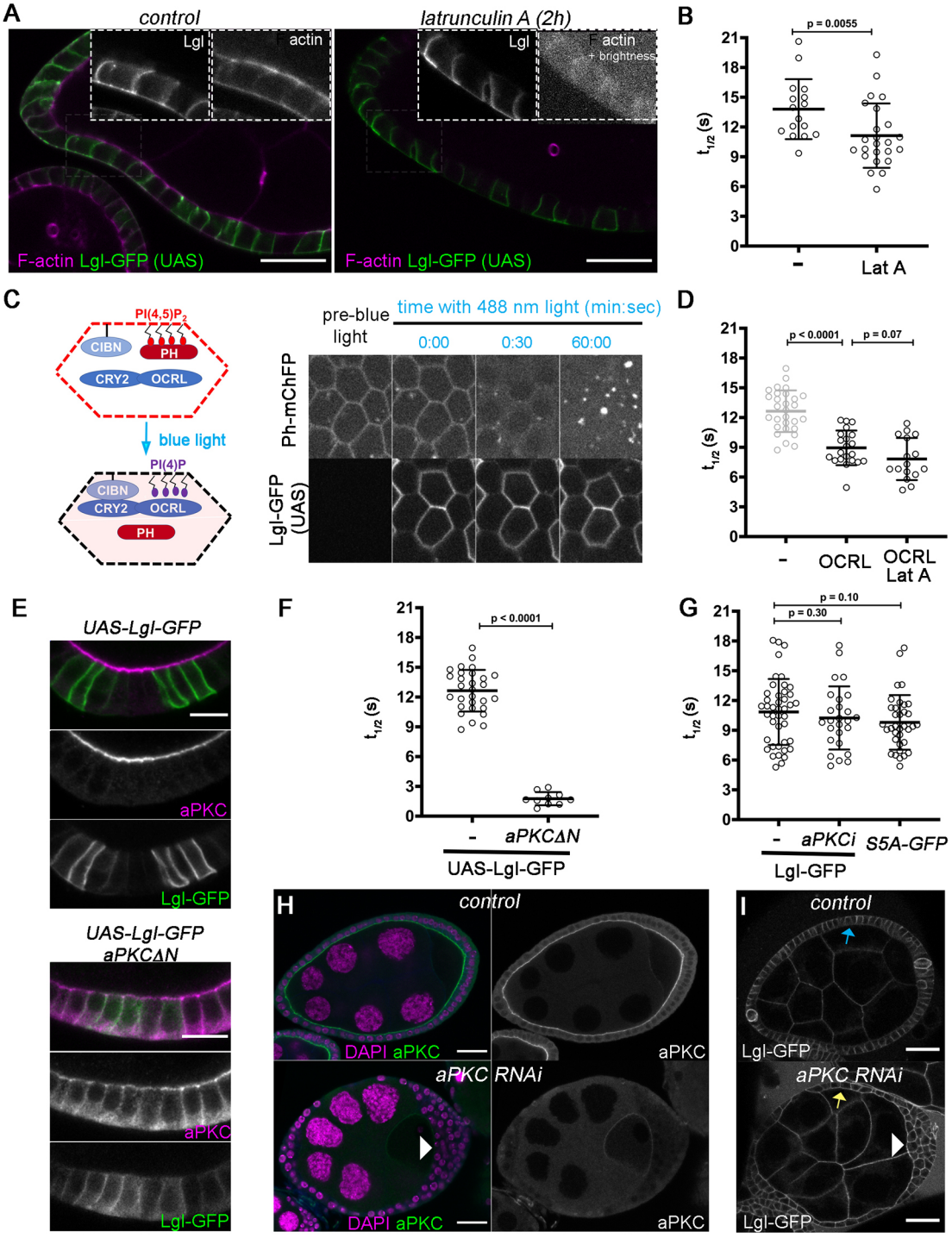

Fig. 2. Lgl dynamics rely on PIP_2 and are independent of aPKC in the lateral cortex. (A) Egg chambers expressing UAS-driven Lgl-GFP were treated with Latrunculin A (LatA). Phalloidin labels F-actin. (B) Scatter plots show Lgl-GFP recovery half-time in control (n=16) and LatA-treated (n=24) egg chambers (mean±s.d.). (C) PIP_2 was depleted by light-dependent recruitment of CRY2 fused with the inositol polyphosphate 5-phosphatase OCRL to CIBN anchored to the plasma membrane. Blue light releases PH-ChFP from the membrane (Movie 2). (D) Half-time distribution (mean±s.d.) of UAS-Lgl-GFP in control (n=29) and PIP_2 depletion alone (OCRL, n=21) or together with LatA (n=16). (E) Follicle cells expressing UAS-Lgl-GFP stained for aPKC. Co-expressing UAS-$aPKC^{\Delta N}$ releases Lgl from the cortex. (F,G) Scatter plots represent half-time of fluorescence recovery for (F) UAS-Lgl-GFP in control (n=29, same dataset as D) and $aPKC^{\Delta N}$-overexpressing cells (n=10), and for (G) endogenously tagged Lgl-GFP (n=43, control), aPKC RNAi (n=26) and Lgl^{S5A}-GFP (homozygous, n=35) (mean±s.d.). (H,I) Midsagittal cross-sections of control and aPKC-depleted egg chambers stained for (H) DAPI and aPKC, or (I) expressing endogenous Lgl-GFP mislocalized to the apical side in aPKC RNAi (arrows). Arrowheads indicate multilayered tissue. Scale bars: 10 µm (E); 25 µm (A,H,I). P-values calculated using the Mann–Whitney U-test.

Thus, the actin cytoskeleton restrains Lgl mobility, possibly through Lgl binding to myosin and other actin cortex-associated proteins (Dahan et al., 2014; Strand et al., 1994).

Mutants for PIP_2 biosynthesis maintain the distribution of apical-basal polarity proteins in the follicular epithelium (Devergne et al., 2014; Khoury and Bilder, 2020), but they can cause defects in

Development (2020) 147, dev186593. doi:10.1242/dev.186593

epithelial architecture (Claret et al., 2014; Devergne et al., 2014). We therefore depleted PIP_2 with high temporal control through light-induced recruitment of the 5-phosphatase OCRL to the plasma membrane, where it converts $PI(4,5)P_2$ to PI(4)P (Guglielmi et al., 2015). This approach triggers efficient removal of PIP_2 sensor PH-ChFP from the plasma membrane, while maintaining cortically localized UAS-driven Lgl-GFP for FRAP analysis (Fig. 2C, Fig. S4). PI(4)P may be sufficient to maintain overexpressed Lgl at the plasma membrane, as previous work shows that co-depletion of PI(4)P with $PI(4,5)P_2$ is required for complete membrane removal (Dong et al., 2015). Importantly, PIP_2 optogenetic depletion accelerates fluorescence recovery in the lateral cortex, supporting the idea that PIP_2 is a major binding partner that restrains Lgl cortical mobility (Fig. 2D). Consistent with this, LatA treatment does not increase Lgl-GFP mobility further when PIP_2 is simultaneously depleted (Fig. 2D).

aPKC-mediated phosphorylation dissociates Lgl from the apical cortex in epithelia (Betschinger et al., 2003; Plant et al., 2003; Yamanaka et al., 2003). aPKC activity at the lateral cortex should promote membrane-cytoplasm exchange by releasing Lgl from plasma membrane phosphoinositides and cortical interactors. Accordingly, ectopic expression of constitutively active $aPKC^{\Delta N}$ (Betschinger et al., 2003) induces cytoplasmic accumulation (Fig. 2E, Fig. S4) and strongly accelerates Lgl-GFP fluorescence recovery at the lateral cortex (Fig. 2F, Fig. S4C). However, Lgl^{S5A}-GFP, a knock-in allele in which all serines phosphorylatable by aPKC are mutated (Dong et al., 2015), shows identical fluorescence recovery to Lgl-GFP (Fig. 2G). Moreover, although aPKC RNAi enables apical accumulation of Lgl, its dynamics are preserved in the lateral cortex (Fig. 2G-I). Thus, aPKC inhibits Lgl accumulation in the apical domain, but has no impact in the lateral cortex, suggesting that aPKC activity is efficiently limited to the apical domain of follicle cells.

Dlg-Scrib regulate Lgl dynamics and localization by preventing aPKC ectopic activity

Scrib and Lgl cortical localization is disrupted in *dlg* mutant follicle cells (Fig. 3A,B, Fig. S5), similar to the *Drosophila* embryonic epithelium (Bilder et al., 2000). However, it is unclear how Dlg and Scrib promote Lgl cortical localization. Loss of Dlg does not interfere with PIP_2-binding sites, as PH-GFP remains unchanged in *dlg* mutant cells (Fig. 3C). Alternatively, mislocalization of aPKC activity in *dlg* cells ((Bilder et al., 2000; Franz and Riechmann, 2010), Fig. 3D) may displace Lgl from the plasma membrane. Accordingly, Lgl^{S5A}-GFP localizes in the cortex of *dlg* mutant clones (Fig. 3E,F, Fig. S5C,D), and an *aPKC* mutation restores Lgl cortical localization in *dlg* mutants (Fig. 3G). This suggests that Dlg is not required for Lgl cortical recruitment in the absence of aPKC phosphorylation. Long-term disruption of aPKC could enable constitutive membrane binding of unphosphorylated Lgl and mask a role for Dlg in Lgl cortical recruitment. We therefore inactivated aPKC acutely using an analogue-sensitive *aPKC* allele (Hannaford et al., 2019). Live imaging of Lgl-GFP shows that aPKC inhibition induces quick reallocation of Lgl from the cytoplasm to the cortex in *dlg* mutant cells (Fig. 3H, Movie 3), indicating that Dlg binding is dispensable for cortical recruitment.

We used FRAP to further test Dlg as a Lgl binding partner. UAS-driven Lgl-GFP enabled us to specifically monitor Lgl cortical dynamics by restoring Lgl cortical localization in *dlg* mutants (Figs S4A,B and S5E). This is consistent with Lgl inhibition of aPKC activity and titration of aPKC activity by overexpression of its substrates (Holly and Prehoda, 2019). UAS-driven Lgl-GFP displays faster fluorescence recovery in the absence of Dlg (Fig. 3I), possibly owing to mislocalized aPKC activity. However, given that Dlg is necessary to localize Scrib, which is also required for Lgl localization (Fig. S5F), this result would also be compatible with Lgl binding to Dlg or Scrib. To determine the specific contribution of Dlg and Scrib as Lgl cortical binding sites versus their impact on the extension of aPKC activity, we measured the dynamics of aPKC-insensitive versions of Lgl in both *dlg* and *scrib* mutants. The dynamic behavior of nonphosphorylatable Lgl is not significantly different in either mutant background (Fig. 3J,K). In contrast, PIP_2 depletion accelerates the fluorescence recovery of nonphosphorylatable Lgl (Fig. 3J,K). We conclude that, whereas Lgl binds to PIP_2 at the plasma membrane, Lgl cortical dynamics are independent of protein-protein interactions with the Scrib-Dlg module.

Dlg-Scrib complex does not contain Lgl in the follicular epithelium

Despite the widespread notion that Dlg, Lgl and Scrib act together, there are no *in vivo* evidences for a tripartite complex. We have recently repurposed light-induced protein clustering by LARIAT [light-activated reversible inhibition by assembled trap (Lee et al., 2014; Qin et al., 2017)] to probe for protein-protein interactions in S2 cells (Osswald et al., 2019). By combining CRY2 tagged with a VHH-GFP nanobody and GFP knock-in lines for Lgl, Dlg and Scrib, we probed for interactions in the follicular epithelium by evaluating co-recruitment to multimeric clusters (Fig. 4A). Light stimulation induced the formation of Scrib-GFP clusters, which accumulate below the adherens junction (Fig. 4B) and contain Dlg (Fig. 4C).

To identify how Dlg binds Scrib, we induced clustering of Scrib versions lacking the leucine-rich repeats (ΔLRR-GFP) or the PDZ domains (ΔPDZ-GFP), which bind the Dlg-binding protein GUK-holder (Caria et al., 2018). Both proteins are largely cytoplasmic and become enriched at the cortex upon clustering, but whereas Dlg is absent from ΔLRR-GFP clusters, Dlg co-clusters with ΔPDZ-GFP (Fig. 4D). Thus, the identified Scrib-Dlg complex is formed by interactions with the LRR-LAPSD domains, which are both essential and partially sufficient for apical-basal polarization and proliferation control in mammalian and *Drosophila* tissues (Choi et al., 2019; Zeitler et al., 2004). We next tested whether Lgl is also included in Dlg-Scrib complexes. In contrast to Scrib-GFP clusters, Dlg is absent from Lgl-GFP clusters (Fig. 4C,E). Conversely, Lgl-mCherry does not colocalize with Scrib-GFP or Dlg-GFP light-induced clusters (Fig. 4F), indicating that Lgl is not part of the Scrib-Dlg complex present in the lateral domain of follicle cells.

Conclusions

Understanding how basolateral proteins maintain apical-basal polarity requires refined approaches to investigate their dynamic behavior, which is intimately connected to function. Dlg and Scrib mobility has previously been studied in septate junctions (Babatz et al., 2018; Oshima and Fehon, 2011). Our study compared the dynamics of the basolateral determinants in the lateral domain and dissected how Lgl associates to the cortex. Lgl dynamics are tightly linked to membrane diffusion, as previously observed for the PIP_2-binding domain PLCδPH (Goehring et al., 2010; Hammond et al., 2009). PIP_2 proteins are indeed major binding sites for Lgl, as previously suggested (Bailey and Prehoda, 2015; Dong et al., 2015). Moreover, even though aPKC phosphorylation induces cortical detachment, we show that aPKC inactivation does not alter Lgl dynamic behavior in the lateral cortex. Thus, there is an efficient restriction of aPKC activity to the apical domain in the steady state of polarized follicle cells. This resembles the maintenance phase of *C. elegans* PAR polarization,

Development (2020) 147, dev186593. doi:10.1242/dev.186593

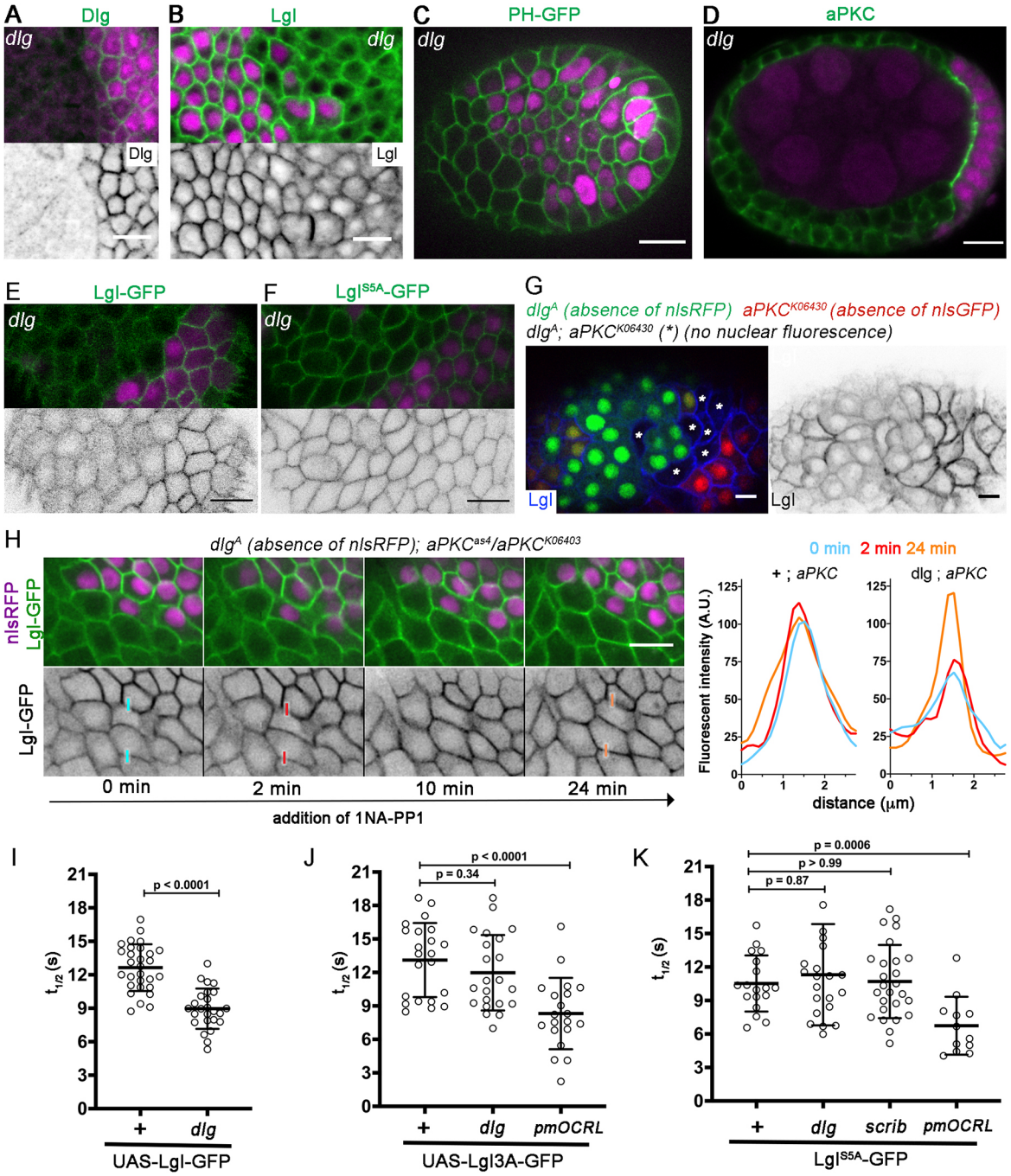

Fig. 3. Dlg and Scrib control Lgl localization and dynamics by preventing ectopic aPKC activity. (A-F) *dlg*^{A} mutant clones [absence of nls-RFP (magenta)] stained for (A) Dlg, (B) Lgl or (D) aPKC, or expressing (C) PLCδPH-GFP, (E) Lgl-GFP or (F) Lgl^{S5A}-GFP. (G) Clonal analysis shows that Lgl cortical localization is disrupted in *dlg*^{A} mutants (green, absence of nlsRFP), but not in double *dlg*^{A}, *aPKC*^{K06403} mutants (asterisk). (H) Time-lapse images of egg chambers expressing the analog-sensitive allele *aPKC*^{as4} treated with 1NA-PP1 (*dlg*^{A} clone marked by absence of nls-RFP). Intensity plots show Lgl-GFP fluorescence (in arbitrary units) across the indicated interfaces of *aPKC*^{as4}/*aPKC*^{K0640} cells that were wild type or *dlg* mutant. (I-K) Scatter plots of recovery half-time ($t_{1/2}$). (I) Accelerated UAS-Lgl-GFP cortical dynamics in *dlg*^{A} (n=25) in comparison with control (n=29). (J) UAS-Lgl^{3A}-GFP dynamics are unchanged in *dlg*^{A} mutants (n=22) and accelerated by PIP_2 optogenetic depletion (n=20) in relation to control (n=22). (K) Lgl^{S5A}-GFP dynamics are maintained in *dlg*^{A} (n=21) and *scrib*^{2} (n=26) in relation to control (n=18), but are accelerated upon PIP_2 depletion (n=12). Data are mean±s.d.. Scale bars: 10 µm. *P*-value calculated with Mann–Whitney U-test.

where the dynamics of PAR proteins are only altered in the region enriched in the opposing species (Goehring et al., 2011).

Although we cannot exclude the possibility that the formation of short-lived protein complexes makes a minor contribution to Lgl dynamics, this study shows that Dlg-Scrib are not major binding partners for Lgl. Instead they regulate cortical Lgl by preventing aPKC ectopic localization and activity in the lateral domain of follicle cells. Our findings are consistent with recent work, which shows that Dlg and Scrib protect Lgl from aPKC in the follicular and embryonic epithelium, possibly by regulation of specific phosphorylation sites (Khoury and Bilder, 2020). This could promote Lgl accumulation at the cortex, and concomitantly prevent aPKC lateral extension by

Development (2020) 147, dev186593. doi:10.1242/dev.186593

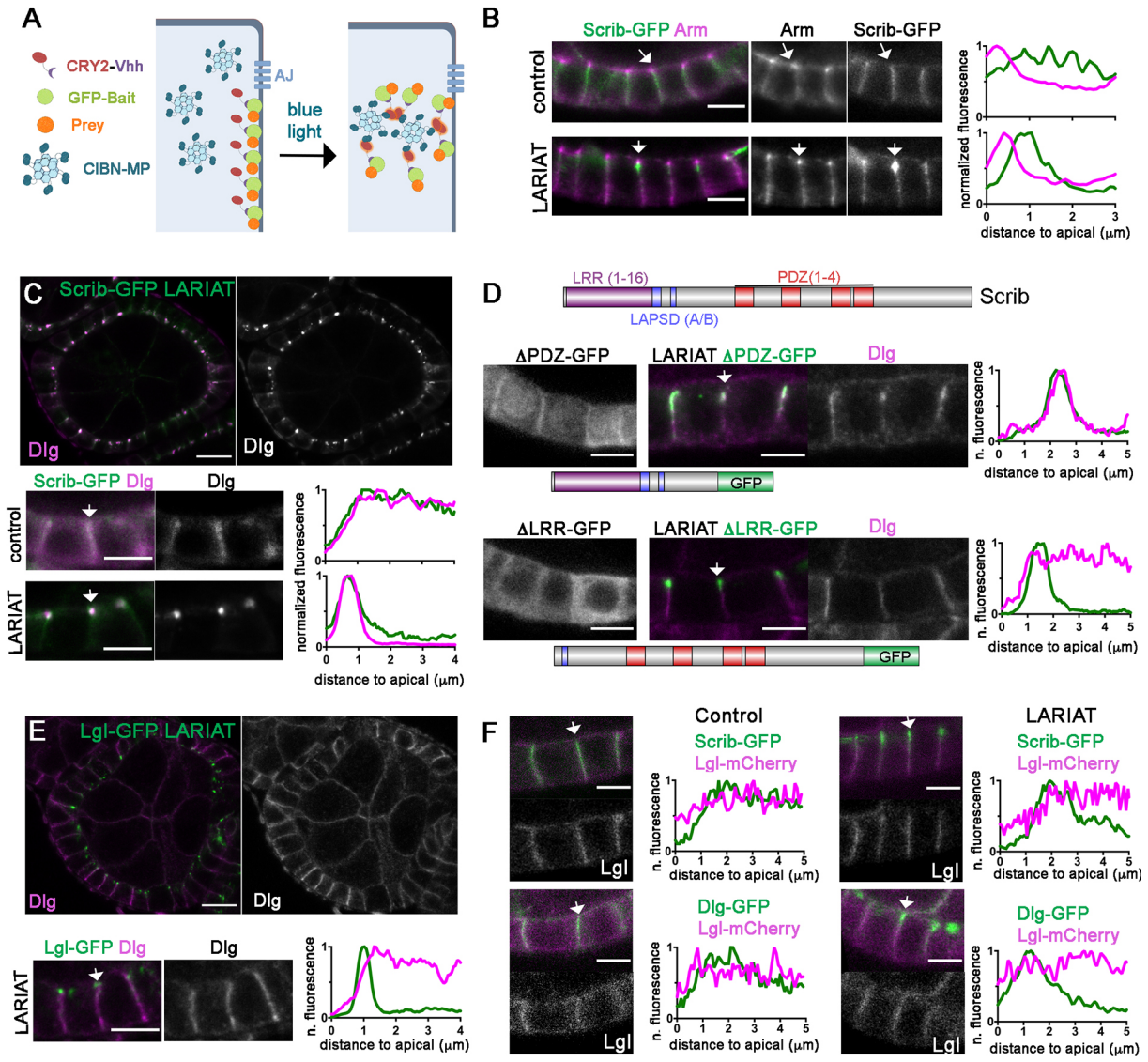

Fig. 4. *In vivo* detection of Scrib-Dlg complexes that lack Lgl. (A) Detection of protein-protein interactions through light-induced clustering. The GFP-tagged protein (bait) binds CRY2-V_HH, which interacts with CIBN-MP upon light exposure to generate multimeric complexes and trap interactors (prey). (B) Light-induced protein clusters of Scribble-GFP localize below Armadillo-stained adherens junctions. (C-E) Dlg immunofluorescence shows co-aggregation with (C) Scribble-GFP, with (D) ScribΔPDZ-GFP but not with Scrib-ΔLRR-GFP or (E) Lgl-GFP. (F) Scribble-GFP and Dlg-GFP do not co-cluster with Lgl-mCherry. (B-F) Pixel intensity profiles were measured along the indicated membranes (arrows) and were normalized to maximum intensity. Scale bars: 5 µm (enlargements); 10 µm (egg chambers in C and E).

inhibiting aPKC-mediated stabilization of apical complexes in the lateral cortex (Fletcher et al., 2012). Moreover, Dlg and Scrib may repress the extension of apical proteins by directing the assembly and location of adherens junctions, as was recently described in the embryonic ectoderm (Bonello et al., 2019). Although further work is necessary to characterize how Dlg-Scrib block apical determination, the separation of function between Scrib-Dlg and Lgl may be conserved as mammalian Scrib orthologues also have Lgl independent roles in epithelial polarity (Choi et al., 2019). In conclusion, this study indicates that Lgl does not act as part of the Scrib-Dlg complex, suggesting individual parallel mechanisms to antagonize apical identity in the follicular epithelium.

MATERIALS AND METHODS

Drosophila stocks and genetics

Stocks used were as follows: *Dlg*^{CC01936}*-GFP*, *Scrib*^{CA07683}*-GFP* (Buszczak et al., 2007), *Lgl-GFP, Lgl*^{S5A}*-GFP* and Lgl-mCherry (Dong et al., 2015) were used for endogenous expression of tagged polarity proteins; *UAS-Lgl*^{3A}*-GFP* and *UAS-Lgl-GFP* (Betschinger et al., 2003) for overexpression conditions; *UAS-pmCIBN* and *UAS-CRY2-OCRL* for optogenetic depletion of PIP_2 in the plasma membrane (Guglielmi et al., 2015; kindly provided by Stephano de Renzis, EMBL, Heidelberg, Germany); UAS-LARIAT (V_hH-SNAPtag-CRY2(PHR)-P2A-CIB1MP) for light-induced clustering of GFP-tagged proteins (Qin et al., 2017; kindly provided by Xiaobo Wang, CBI, Toulouse, France), including *UAS-ScribΔLRR-GFP* (BDSC: #59084) and *UAS-ScribΔPDZ-GFP* (BDSC: #59083); UAS- *PLCδPH-GFP* (BDSC: #39693), *ubi-PLCγPH-eGFP* or *ubi-PLCγPH-mCherry* (PH-ChFP) (Herszterg et al., 2013; kindly provided by Yohanns Bellaiche, Institut Curie, Paris, France) was used to label PIP_2 with the pleckstrin homology (PH) domain of PLCγ; *UAS-aPKC RNAi* (BDSC: #25946); *UAS aPKC*$^{\Delta N}$ (Betschinger et al., 2003); *aPKC*^{K06403} (Wodarz et al., 2000); *apkc*^{as4}, an analogue-sensitive allele used for acute inhibition of aPKC (Hannaford et al., 2019; kindly provided by Jens Januschke, University of Dundee, UK); and *scrib*^{2} (Bilder and Perrimon, 2000). We used a recently generated *dlg*^{A} mutant allele, which was produced with low concentrations of ethyl

Development (2020) 147, dev186593. doi:10.1242/dev.186593

methylsulphonate, to diminish secondary alterations (Haelterman et al., 2014; Yamamoto et al., 2014). *dlg*^{A} encodes a stop codon on the third PDZ domain of Dlg and behaves as a protein null allele. Mitotic clones were generated with the FLP/FRT-mediated mitotic recombination system and were induced by heat shock at 37°C (Xu and Rubin, 1993).

Drosophila melanogaster stocks were reared on standard cornmeal/agar/molasses/yeast media at 18°C or 25°C. To boost UAS-RNAi or UAS-LARIAT expression, flies were raised at 29°C overnight. Flies were protected from the light before light induction in the optogenetic experiments. *tj-GAL4* and *GR1-GAL4* were used to drive the expression of UAS transgenes in the follicular epithelium.

Genotypes

FRAP analysis of *UAS-Lgl-GFP*

tj-GAL4/+; *UAS-Lgl-GFP*/+ (Figs 2A,B,I and 3I)
tj-GAL4/+; *UAS aPKC*$^{\Delta N}$*/UAS-Lgl-GFP* (Fig. 2E,F)

FRAP analysis of *PLCδPH-GFP*

tj-GAL4/+; *UAS-PLCδPH-GFP*/+ (Fig. S2)

Lgl^{S5A} homozygous

hs-FLP; *Lgl*^{S5A}*-GFP FRT40A/nls-RFP FRT40A* (Fig. 2G)

Lgl-GFP in aPKC RNAi

tj-GAL4, Lgl-GFP/, Lgl-GFP; *UAS aPKC RNAi*/ (Fig. 2G,I)

aPKC RNAi

tj-GAL4/+; *UAS aPKC RNAi*/+ (Fig. 2H)

Optogenetic PIP_2 depletion

UAS-*pmCIBN/UAS-CRY2-OCRL*; *tj-GAL4*/+; *ubi-PH-mCherry*/+; *UAS-Lgl-GFP*/+ (Fig. 2C,D)
UAS-*pmCIBN/UAS-CRY2-OCRL*; *tj-GAL4*/+; *ubi-PH-mCherry*/+; *UAS-Lgl*^{3A}*-GFP*/+ (Fig. 3J)
UAS-*pmCIBN/UAS-CRY2-OCRL*; *tj-GAL4*/+; Lgl^{5A}-GFP/ubi-PH-mCherry (Fig. 3K)

dlg mutant clones

dlg^{A} *FRT19A/hs-FLP nls-RFP FRT19A* (Fig. 3A,B,D)
dlg^{A} *FRT19A/hs-FLP nls-RFP FRT19A*;; *ubi-PH-mCherry* (Fig. 3C)
dlg^{A} *FRT19A/hs-FLP nls-RFP FRT19A*; *tj-GAL4*/+; *UAS-Lgl-GFP*/+ (Fig. 3I and Fig. S4A,B)
dlg^{A} *FRT19A/hs-FLP nls-RFP FRT19A*; *tj-GAL4*/+; *UAS-Lgl*^{3A}*-GFP*/+ (Fig. 3J)
dlg^{A} *FRT19A/hs-FLP nls-RFP FRT19A*; *Lgl*^{5A}*-GFP*/+ (Fig. 3F,K, Fig. S5D)
dlg^{A} *FRT19A/hs-FLP nls-RFP FRT19A*; *Lgl-GFP* (Fig. 3E, Fig. S5C)
dlg^{A} *FRT19/hs-FLP nls-RFP FRT19A*;; *Scrib-GFP* (Fig. S5A,B)

Double *dlg,aPKC* mutants

dlg^{A} *FRT19A/hs-FLP nls-RFP FRT19A*; *FRT42B aPKC*^{K06430}*/FRT42B nls-GFP* (Fig. 3G)
dlg^{A} *FRT19/hs-FLP nls-RFP FRT19A*; *Lgl-GFP aPKC*^{K06403}*/aPKC*^{as4} (Fig. 3H)

scrib mutant clones:

hs-FLP/+; *Lgl*^{S5A}*-GFP/+*; *FRT82 RFP/FRT82 scrib*^{2} (Fig. 3K)
hs-FLP/+; *Lgl-GFP/+*; *FRT82 RFP/FRT82 scrib*^{2} (Fig. S5F)

LARIAT optogenetic clustering experiments

tj-GAL4 or *UAS-LARIAT/Cyo*; *Scrib-GFP/TM6* (control) (Fig. 4B)
tj-GAL4/UAS-LARIAT; *Scrib-GFP/TM6* (Fig. 4B)
tj-GAL4 or UAS-LARIAT/Cyo; *Scrib-GFP/Scrib-GFP* (control) (Fig. 4C)
tj-GAL4/UAS-LARIAT; *Scrib-GFP/Scrib-GFP* (Fig. 4C)
UAS-ScribΔPDZ-GFP/Cyo; *UAS-LARIAT GR1-GAL4*/+ (Fig. 4D)
UAS-ScribΔLRR-GFP/UAS-LARIAT GR1-GAL4 (Fig. 4D)
tj-GAL4/ Lgl-GFP; *UAS-LARIAT GR1-GAL4*/+ (Fig. 4E)
Lgl-mCherry/Cyo; *UAS-LARIAT/ Scrib-GFP* (control) (Fig. 4F)
tj-GAL4/Lgl-mCherry; *UAS-LARIAT/Scrib-GFP* (Fig. 4F)
Dlg-GFP/+; *tj-GAL4/Lgl-mCherry*; *TM6/+* (Fig. 4F)
Dlg-GFP/+; *tj-GAL4/Lgl-mCherry*; *UAS-LARIAT/+* (Fig. 4F)

Immunofluorescence

Ovaries of well-fed *Drosophila* females were fixed in 4% paraformaldehyde (in PBS) for 20 min, washed 3×10 min in PBT (PBS with 0.05% of Tween 20), blocked with PBT-10 (PBT supplemented with 10% BSA) and then incubated overnight with primary antibodies in PBT supplemented with 1% BSA. After 4×30 min washes in PBT, ovaries were incubated with a secondary antibody for 2 h, washed three times for 10 min with PBT and mounted in Vectashield with DAPI (Vector Laboratories). The following primary antibodies were used: rabbit anti-Lgl (1:100, d-300, Santa Cruz Biotechnology), rabbit anti-aPKC (1:500, c-20, Santa Cruz Biotechnology) and mouse anti-Dlg (1:200, F3 Developmental Studies Hybridoma Bank). Fixed tissue was imaged using a 1.1 numerical aperture/40× water or 1.30 numerical aperture/63× objectives on an inverted laser scanning confocal microscope Leica TCS SP5 II (Leica Microsystems) or with a 1.20 numerical aperture/63× objective on an inverted laser scanning confocal microscope Leica TCS SP8 (Leica Microsystems).

Drug treatments

Actin cytoskeleton disruption was achieved by treating dissected ovarioles for at least 1 h with 5 µg/ml of Latrunculin A (Sigma-Aldrich) added to the Imaging Medium [Schneider Insect Cell Medium (Gibco) supplemented with 10% FBS (ThermoFisher) and 200 µg/µl of Insulin (Sigma)]. Temporal inhibition of aPKC activity in *dlg* mutant cells was achieved by using flies carrying simultaneously the *apkc*^{as} allele by addition of 1NA-PP1 (Calbiochem) to the imaging media at a final concentration of 100 µM immediately before imaging.

Optogenetic experiments

Flies were exposed for 24 h to direct blue LED light (472 nm) prior to ovary dissection and fixation to trigger GFP-tagged protein clustering. For optogenetic depletion of PIP_2 by the inositol polyphosphate 5-phosphatase OCRL, ovaries were dissected using a 593 nm LED light and exposed to a 488 nm laser during the live imaging process. FRAP experiments were performed between ∼5 min and 1 h after optogenetic activation.

Fluorescence recovery after photobleaching in the *Drosophila* follicular epithelium

Drosophila egg chambers from stage 7 to stage 9 were imaged in culture dishes (MatTek) with either Imaging Medium (Prasad et al., 2007) or with 10S Voltalef oil (VWR Chemicals). Imaging Medium was used for experiments with overexpressed GFP-tagged proteins. We resorted to the better optical properties of 10S Voltalef to improve the fluorescence signal-to-noise ratio in the experiments using endogenously tagged-GFP proteins. FRAP experiments were performed using a 1.1 numerical aperture/40× water objective on a Leica TCS SP5 II (Leica Microsystems) confocal microscope and using the FRAP Wizard application of the LAS Advance Fluorescence (AF) 2.6. software. The imaging plane was focused at the surface of the egg chamber on the lateral cortex of the follicular epithelium (Fig. S1A), where a cortical section of two neighboring cells was selected for bleaching using either a rectangular ROI of 3 µm×1.0 µm. A 1.5 µm×1 µm ROI during the bleaching process was used to determine whether diffusion played a role in Lgl recovery (Fig. 1E).

For all the FRAP experiments performed, a three-step protocol was developed: (1) a pre-bleaching acquisition phase for GFP equilibration; (2) a photoperturbation step performed using a single bleaching pulse with the 405 laser line (50 mW) at maximum laser power using the Zoom In option of the FRAP Wizard; and (3) post-bleaching phases to measure the fluorescence recovery. Pre- and post-bleach imaging of GFP was performed using the 488 nm excitation line with 20%-35% laser intensity. The multi-step FRAP protocol was optimized for each basolateral polarity protein (Fig. 1A), ensuring that sufficient data points were collected to accurately obtain the half-time of recovery while minimizing photobleaching during

Development (2020) 147, dev186593. doi:10.1242/dev.186593

acquisition: pre-bleaching, six frames acquired for equilibration of GFP signal (0.543 s between frames); post-bleaching 1 (1 s/frame) Lgl, 25 frames; Dlg, 50 frames; Scrib, 60 frames; PH; 30 frames; post-bleaching 2 (3 s/frame) Lgl, 25 frames; Dlg, 50 frames; Scrib, 60 frames; PH; 10 frames; and post-bleaching 3 (10 s/frame) Lgl, 10 frames; Dlg, 30 frames; Scrib, 35 frames.

Image processing and fluorescence recovery curve normalization

Image processing and fluorescence intensity recovery measuring were performed using ImageJ (Schindelin et al., 2012) (http://imagej.nih.gov/ij/) through a pipeline composed of three main steps.

(1) Registering the timelapse images

Image drift during acquisition was corrected using the 'Stack Reg' plug-in to align time lapse images.

(2) Measuring the raw fluorescence intensity values from the corrected images

Measurements were collected in four different regions: (1) 3 µm×1 µm ROI containing the photobleached region (Bl in Fig. S1A); (2 and 3) two 3 µm×1.5 µm ROIs in cortical regions (NB in Fig. S1A) non-adjacent to the photobleached region to correct for photobleaching during the acquisition of post-bleaching steps; and (4) a 2 µm diameter circular ROI placed in the prospective nucleus, used for background subtraction as none of the proteins of interest is present in the nucleus (B in Fig. S1A). We note that 1 µm diameter cytoplasmic ROIs were used to determine cytoplasmic intensity of Lgl.

(3) Subtracting the background, correcting for photobleaching during acquisition and normalizing recovery data

We obtain the corrected and normalized data (%F(t)) by applying Eqn 1. In this equation, background subtracted intensities in the bleached ROI (Bl) were normalized to the mean of the three pre-bleaching (pre) frames and corrected for acquisition photobleaching using the mean of the background subtracted intensities of two non-bleached ROI (NB). The fluorescence recovery curve is presented as a percentage of the pre-bleach intensity, and the value of the first frame post-bleach, $Bl(t_0)$, is set to zero to obtain recovery curves that enable comparison of experiments with different bleaching depths.

$$\%F(t) = \frac{Bl(t) - Bl(t_0)}{Bl(pre) - Bl(t_0)} \times \frac{NB(pre)}{NB(t)} \times 100. \quad \text{(Eqn 1)}$$

Data analysis and statistics

The corrected and normalized data was plotted in recovery curves using GraphPad Prism 8.2.0. Recovery plots represent the average normalized fluorescence intensity and error bars indicate 95% confidence intervals (CI). We performed an extra sum-of-squares F test to assess the preferred model (bi-exponential versus single-exponential) of each individual curve obtained for Lgl-GFP fluorescence recovery. Although bi-exponential fitting was predominantly the best model for the individual Lgl-GFP fluorescence recovery curves (79%, n=43), the bi-exponential model produced open-ended 95% confidence intervals for half-times or a plateau for a large fraction of these curves (28%). Moreover, one-exponential was the preferred model for another fraction of the curves (21%). For Fig. 1E, values were fitted to a bi-exponentional function: $F(t) = Span_{Fast} \times (1 - \exp(-K_{Fast} \times t)) + Span_{Slow} \times (1 - \exp(-K_{Slow} \times t))$, where $Span_{fast}$ and $Span_{slow}$ are the amplitudes of the fast and slow fractions of recovery (constrained to a shared value between the individual curves of a single dataset), and K_{slow} and K_{fast} are rate constants expressed in reciprocal of the time. This function allows to calculate the fast half-time [$t_{fast}=\ln(2)/K_{fast}$] and the slow half-time [$t_{slow}=\ln(2)/K_{slow}$]. Because we concluded that we could not separate membrane diffusion from membrane-cytoplasm exchange using the double exponential equation, we used a single exponential function for individual curve fitting to compare the recovery half-times of Lgl dynamics in different experimental settings: $F(t) = Plateau \times (1 - \exp(-Kd \times t))$, where K_d represents the rate of the unbinding reaction expressed in reciprocal of the time. This function allows us to extract a simple half-time value ($t_{1/2}$) for each curve representing one cell [$t_{1/2}=\ln(2)/kd$]. We then obtained and compared half-time dispersion plots for the different biological conditions. The statistical significance between them was assessed using the non-parametric Mann–Whitney U-test.

Individual photobleaching experiments were excluded from the experimental datasets if they met one of the following criteria: (1) inefficient photobleaching step, such that reduction of intensity in the photobleached region after the bleaching pulse was below 50% (the recommended minimum for quantitative analysis of FRAP curves; McNally, 2008); (2) low plateau of fluorescence recovery [cutoff at 65% (60% for Lgl^{S5A}-GFP+pmOCRL and UAS-Lgl-GFP+$aPKC^{\Delta N}$ to correct for lower plateau in the average of the whole dataset]; (3) values with low R^2 [cutoff at 0.75 (0.65 for Lgl^{S5A}-GFP+pmOCRL and UAS-Lgl-GFP+$aPKC^{\Delta N}$)] (Mean values of the collected data are shown in Table S1.); (4) the half-time of recovery is an outlier (outliers were removed using the Extreme Studentized Method (ESD Method) with a significance level of 0.05 using a GraphPad online application (http://www.graphpad.com/quickcalcs/Grubbs1.cfm).

Acknowledgements

We thank J. Januschke, J. Knoblich, S. De Renzis, Y. Bellaiche, X. Wang, D. St Johnston and the Bloomington stock center for fly stocks. We thank H. Richardson for detailed information on the Scrib-GFP deletion constructs, Y. Bellaiche for comments on the manuscript and C. Sunkel for assistance with supervision.

Competing interests

The authors declare no competing or financial interests.

Author contributions

Conceptualization: G.V., S.M., E.M.-d-S.; Methodology: G.V., S.M., A.B.-C., M.O., E.M.-d-S.; Formal analysis: G.V., S.M., A.B.-C., E.M.-d-S.; Investigation: G.V., S.M., A.B.-C., M.O.; Writing - original draft: E.M.-d-S.; Writing - review & editing: G.V., S.M., M.O., E.M.-d-S.; Supervision: E.M.-d-S.; Project administration: E.M.-d-S.; Funding acquisition: E.M.-d-S.

Funding

This work was supported by Fundação para a Ciência e a Tecnologia (PTDC/BEX-BCM/0432/2014).

Supplementary information

Supplementary information available online at
https://dev.biologists.org/lookup/doi/10.1242/dev.186593.supplemental

Peer review history

The peer review history is available online at
https://dev.biologists.org/lookup/doi/10.1242/dev.186593.reviewer-comments.pdf

References

Atwood, S. X. and Prehoda, K. E. (2009). aPKC phosphorylates miranda to polarize fate determinants during neuroblast asymmetric cell division. *Curr. Biol.* **19**, 723-729. doi:10.1016/j.cub.2009.03.056

Babatz, F., Naffin, E. and Klämbt, C. (2018). The Drosophila blood-brain barrier adapts to cell growth by unfolding of pre-existing septate junctions. *Dev. Cell* **47**, 697-710.e3. doi:10.1016/j.devcel.2018.10.002

Bailey, M. J. and Prehoda, K. E. (2015). Establishment of par-polarized cortical domains via phosphoregulated membrane motifs. *Dev. Cell* **35**, 199-210. doi:10.1016/j.devcel.2015.09.016

Beatty, A., Morton, D. and Kemphues, K. (2010). The C. elegans homolog of Drosophila lethal giant larvae functions redundantly with PAR-2 to maintain polarity in the early embryo. *Development* **137**, 3995-4004. doi:10.1242/dev.056028

Bell, G. P., Fletcher, G. C., Brain, R. and Thompson, B. J. (2015). Aurora kinases phosphorylate Lgl to induce mitotic spindle orientation in Drosophila epithelia. *Curr. Biol.* **25**, 61-68. doi:10.1016/j.cub.2014.10.052

Bergstralh, D. T., Lovegrove, H. E. and St Johnston, D. (2013). Discs large links spindle orientation to apical-basal polarity in Drosophila epithelia. *Curr. Biol.* **23**, 1707-1712. doi:10.1016/j.cub.2013.07.017

Betschinger, J., Mechtler, K. and Knoblich, J. A. (2003). The par complex directs asymmetric cell division by phosphorylating the cytoskeletal protein Lgl. *Nature* **422**, 326-330. doi:10.1038/nature01486

Betschinger, J., Eisenhaber, F. and Knoblich, J. A. (2005). Phosphorylation-induced autoinhibition regulates the cytoskeletal protein lethal (2) giant larvae. *Curr. Biol.* **15**, 276-282. doi:10.1016/j.cub.2005.01.012

Bilder, D., Li, M. and Perrimon, N. (2000). Cooperative regulation of cell polarity and growth by Drosophila tumor suppressors. *Science* **289**, 113-116. doi:10.1126/science.289.5476.113

Bilder, D., Schober, M. and Perrimon, N. (2003). Integrated activity of PDZ protein complexes regulates epithelial polarity. *Nat. Cell Biol.* **5**, 53-58. doi:10.1038/ncb897

Bonello, T. T. and Peifer, M. (2019). Scribble: a master scaffold in polarity, adhesion, synaptogenesis, and proliferation. *J. Cell Biol.* **218**, 742-756. doi:10.1083/jcb.201810103

Bonello, T. T., Choi, W. and Peifer, M. (2019). Scribble and discs-large direct initial assembly and positioning of adherens junctions during the establishment of apical-basal polarity. *Development* **146**, dev180976. doi:10.1242/dev.180976

Buszczak, M., Paterno, S., Lighthouse, D., Bachman, J., Planck, J., Owen, S., Skora, A. D., Nystul, T. G., Ohlstein, B., Allen, A. et al. (2007). The carnegie protein trap library: a versatile tool for Drosophila developmental studies. *Genetics* **175**, 1505-1531. doi:10.1534/genetics.106.065961

Caria, S., Magtoto, C. M., Samiei, T., Portela, M., Lim, K. Y. B., How, J. Y., Stewart, B. Z., Humbert, P. O., Richardson, H. E. and Kvansakul, M. (2018). Drosophila melanogaster Guk-holder interacts with the Scribbled PDZ1 domain and regulates epithelial development with scribbled and discs large. *J. Biol. Chem.* **293**, 4519-4531. doi:10.1074/jbc.M117.817528

Carvalho, C. A., Moreira, S., Ventura, G., Sunkel, C. E. and Morais-de-Sá, E. (2015). Aurora A triggers Lgl cortical release during symmetric division to control planar spindle orientation. *Curr. Biol.* **25**, 53-60. doi:10.1016/j.cub.2014.10.053

Chalmers, A. D., Pambos, M., Mason, J., Lang, S., Wylie, C. and Papalopulu, N. (2005). aPKC, Crumbs3 and Lgl2 control apicobasal polarity in early vertebrate development. *Development* **132**, 977-986. doi:10.1242/dev.01645

Chen, J., Sayadian, A.-C., Lowe, N., Lovegrove, H. E. and St Johnston, D. (2018). An alternative mode of epithelial polarity in the Drosophila midgut. *PLoS Biol.* **16**, e3000041. doi:10.1371/journal.pbio.3000041

Choi, J., Troyanovsky, R. B., Indra, I., Mitchell, B. J. and Troyanovsky, S. M. (2019). Scribble, erbin, and lano redundantly regulate epithelial polarity and apical adhesion complex. *J. Cell Biol.* **218**, 2277-2293. doi:10.1083/jcb.201804201

Claret, S., Jouette, J., Benoit, B., Legent, K. and Guichet, A. (2014). PI(4,5)P2 produced by the PI4P5K SKTL controls apical size by tethering PAR-3 in Drosophila epithelial cells. *Curr. Biol.* **24**, 1071-1079. doi:10.1016/j.cub.2014.03.056

Dahan, I., Petrov, D., Cohen-Kfir, E. and Ravid, S. (2014). The tumor suppressor Lgl1 forms discrete complexes with NMII-A and Par6alpha-aPKCzeta that are affected by Lgl1 phosphorylation. *J. Cell Sci.* **127**, 295-304. doi:10.1242/jcs.127357

Devergne, O., Tsung, K., Barcelo, G. and Schupbach, T. (2014). Polarized deposition of basement membrane proteins depends on Phosphatidylinositol synthase and the levels of Phosphatidylinositol 4,5-bisphosphate. *Proc. Natl. Acad. Sci. USA* **111**, 7689-7694. doi:10.1073/pnas.1407351111

Dong, W., Zhang, X., Liu, W., Chen, Y.-J., Huang, J., Austin, E., Celotto, A. M., Jiang, W. Z., Palladino, M. J., Jiang, Y. et al. (2015). A conserved polybasic domain mediates plasma membrane targeting of Lgl and its regulation by hypoxia. *J. Cell Biol.* **211**, 273-286. doi:10.1083/jcb.201503067

Dow, L. E., Brumby, A. M., Muratore, R., Coombe, M. L., Sedelies, K. A., Trapani, J. A., Russell, S. M., Richardson, H. E. and Humbert, P. O. (2003). hScrib is a functional homologue of the Drosophila tumour suppressor Scribble. *Oncogene* **22**, 9225-9230. doi:10.1038/sj.onc.1207154

Fichelson, P., Jagut, M., Lepanse, S., Lepesant, J.-A. and Huynh, J.-R. (2010). lethal giant larvae is required with the par genes for the early polarization of the Drosophila oocyte. *Development* **137**, 815-824. doi:10.1242/dev.045013

Fletcher, G. C., Lucas, E. P., Brain, R., Tournier, A. and Thompson, B. J. (2012). Positive feedback and mutual antagonism combine to polarize crumbs in the Drosophila follicle cell epithelium. *Curr. Biol.* **22**, 1116-1122. doi:10.1016/j.cub.2012.04.020

Flores-Benitez, D. and Knust, E. (2016). Dynamics of epithelial cell polarity in Drosophila: how to regulate the regulators? *Curr. Opin. Cell Biol.* **42**, 13-21. doi:10.1016/j.ceb.2016.03.018

Franz, A. and Riechmann, V. (2010). Stepwise polarisation of the Drosophila follicular epithelium. *Dev. Biol.* **338**, 136-147. doi:10.1016/j.ydbio.2009.11.027

Fritzsche, M. and Charras, G. (2015). Dissecting protein reaction dynamics in living cells by fluorescence recovery after photobleaching. *Nat. Protoc.* **10**, 660-680. doi:10.1038/nprot.2015.042

Gateff, E. (1978). Malignant neoplasms of genetic origin in Drosophila melanogaster. *Science* **200**, 1448-1459. doi:10.1126/science.96525

Goehring, N. W., Chowdhury, D., Hyman, A. A. and Grill, S. W. (2010). FRAP analysis of membrane-associated proteins: lateral diffusion and membrane-cytoplasmic exchange. *Biophys. J.* **99**, 2443-2452. doi:10.1016/j.bpj.2010.08.033

Goehring, N. W., Hoege, C., Grill, S. W. and Hyman, A. A. (2011). PAR proteins diffuse freely across the anterior-posterior boundary in polarized C. elegans embryos. *J. Cell Biol.* **193**, 583-594. doi:10.1083/jcb.201011094

Grifoni, D., Garoia, F., Bellosta, P., Parisi, F., De Biase, D., Collina, G., Strand, D., Cavicchi, S. and Pession, A. (2007). aPKCzeta cortical loading is associated with Lgl cytoplasmic release and tumor growth in Drosophila and human epithelia. *Oncogene* **26**, 5960-5965. doi:10.1038/sj.onc.1210389

Guglielmi, G., Barry, J. D., Huber, W. and De Renzis, S. (2015). An optogenetic method to modulate cell contractility during tissue morphogenesis. *Dev. Cell* **35**, 646-660. doi:10.1016/j.devcel.2015.10.020

Haelterman, N. A., Jiang, L., Li, Y., Bayat, V., Sandoval, H., Ugur, B., Tan, K. L., Zhang, K., Bei, D., Xiong, B. et al. (2014). Large-scale identification of chemically induced mutations in Drosophila melanogaster. *Genome Res.* **24**, 1707-1718. doi:10.1101/gr.174615.114

Hammond, G. R. V., Sim, Y., Lagnado, L. and Irvine, R. F. (2009). Reversible binding and rapid diffusion of proteins in complex with inositol lipids serves to coordinate free movement with spatial information. *J. Cell Biol.* **184**, 297-308. doi:10.1083/jcb.200809073

Hannaford, M., Loyer, N., Tonelli, F., Zoltner, M. and Januschke, J. (2019). A chemical-genetics approach to study the role of atypical protein kinase C in Drosophila. *Development* **146**, dev170589. doi:10.1242/dev.170589

Herszterg, S., Leibfried, A., Bosveld, F., Martin, C. and Bellaiche, Y. (2013). Interplay between the dividing cell and its neighbors regulates adherens junction formation during cytokinesis in epithelial tissue. *Dev. Cell* **24**, 256-270. doi:10.1016/j.devcel.2012.11.019

Hoege, C., Constantinescu, A.-T., Schwager, A., Goehring, N. W., Kumar, P. and Hyman, A. A. (2010). LGL can partition the cortex of one-cell Caenorhabditis elegans embryos into two domains. *Curr. Biol.* **20**, 1296-1303. doi:10.1016/j.cub.2010.05.061

Holly, R. W. and Prehoda, K. E. (2019). Phosphorylation of Par-3 by atypical protein kinase C and competition between its substrates. *Dev. Cell* **49**, 678-679. doi:10.1016/j.devcel.2019.05.002

Hutterer, A., Betschinger, J., Petronczki, M. and Knoblich, J. A. (2004). Sequential roles of Cdc42, Par-6, aPKC, and Lgl in the establishment of epithelial polarity during Drosophila embryogenesis. *Dev. Cell* **6**, 845-854. doi:10.1016/j.devcel.2004.05.003

Kallay, L. M., McNickle, A., Brennwald, P. J., Hubbard, A. L. and Braiterman, L. T. (2006). Scribble associates with two polarity proteins, Lgl2 and Vangl2, via distinct molecular domains. *J. Cell. Biochem.* **99**, 647-664. doi:10.1002/jcb.20992

Khoury, M. J. and Bilder, D. (2020). Distinct activities of scrib module proteins organize epithelial polarity. *Proc. Natl. Acad. Sci. USA* **117**, 11531-11540. doi:10.1101/866863

Lee, S., Park, H., Kyung, T., Kim, N. Y., Kim, S., Kim, J. and Heo, W. D. (2014). Reversible protein inactivation by optogenetic trapping in cells. *Nat. Methods* **11**, 633-636. doi:10.1038/nmeth.2940

Legouis, R., Jaulin-Bastard, F., Schott, S., Navarro, C., Borg, J. P. and Labouesse, M. (2003). Basolateral targeting by leucine-rich repeat domains in epithelial cells. *EMBO Rep.* **4**, 1096-1102. doi:10.1038/sj.embor.7400006

McMahon, L., Legouis, R., Vonesch, J. L. and Labouesse, M. (2001). Assembly of C. elegans apical junctions involves positioning and compaction by LET-413 and protein aggregation by the MAGUK protein DLG-1. *J. Cell Sci.* **114**, 2265-2277.

McNally, J. G. (2008). Quantitative FRAP in analysis of molecular binding dynamics in vivo. *Methods Cell Biol.* **85**, 329-351. doi:10.1016/S0091-679X(08)85014-5

Moreira, S., Osswald, M., Ventura, G., Gonçalves, M., Sunkel, C. E. and Morais-de-Sa, E. (2019). PP1-Mediated Dephosphorylation of Lgl Controls Apical-basal Polarity. *Cell Rep.* **26**, 293-301.e7. doi:10.1016/j.celrep.2018.12.060

Müsch, A., Cohen, D., Yeaman, C., Nelson, W. J., Rodriguez-Boulan, E. and Brennwald, P. J. (2002). Mammalian homolog of Drosophila tumor suppressor lethal (2) giant larvae interacts with basolateral exocytic machinery in Madin-Darby canine kidney cells. *Mol. Biol. Cell* **13**, 158-168. doi:10.1091/mbc.01-10-0496

Nakajima, Y.-I., Meyer, E. J., Kroesen, A., McKinney, S. A. and Gibson, M. C. (2013). Epithelial junctions maintain tissue architecture by directing planar spindle orientation. *Nature* **500**, 359-362. doi:10.1038/nature12335

Nakajima, Y.-I., Lee, Z. T., McKinney, S. A., Swanson, S. K., Florens, L. and Gibson, M. C. (2019). Junctional tumor suppressors interact with 14-3-3 proteins to control planar spindle alignment. *J. Cell Biol.* **218**, 1824-1838. doi:10.1083/jcb.201803116

Ohshiro, T., Yagami, T., Zhang, C. and Matsuzaki, F. (2000). Role of cortical tumour-suppressor proteins in asymmetric division of Drosophila neuroblast. *Nature* **408**, 593-596. doi:10.1038/35046087

Oshima, K. and Fehon, R. G. (2011). Analysis of protein dynamics within the septate junction reveals a highly stable core protein complex that does not include the basolateral polarity protein Discs large. *J. Cell Sci.* **124**, 2861-2871. doi:10.1242/jcs.087700

Osswald, M., Santos, A. F. and Morais-de-Sá, E. (2019). Light-induced protein clustering for optogenetic interference and protein interaction analysis in Drosophila S2 cells. *Biomolecules* **9**, 61. doi:10.3390/biom9020061

Peng, C.-Y., Manning, L., Albertson, R. and Doe, C. Q. (2000). The tumour-suppressor genes lgl and dlg regulate basal protein targeting in Drosophila neuroblasts. *Nature* **408**, 596-600. doi:10.1038/35046094

Plant, P. J., Fawcett, J. P., Lin, D. C. C., Holdorf, A. D., Binns, K., Kulkarni, S. and Pawson, T. (2003). A polarity complex of mPar-6 and atypical PKC binds, phosphorylates and regulates mammalian Lgl. *Nat. Cell Biol.* **5**, 301-308. doi:10.1038/ncb948

Prasad, M., Jang, A. C.-C., Starz-Gaiano, M., Melani, M. and Montell, D. J. (2007). A protocol for culturing Drosophila melanogaster stage 9 egg chambers for live imaging. *Nat. Protoc.* **2**, 2467-2473. doi:10.1038/nprot.2007.363

Qin, X., Park, B. O., Liu, J., Chen, B., Choesmel-Cadamuro, V., Belguise, K., Heo, W. D. and Wang, X. (2017). Cell-matrix adhesion and cell-cell adhesion differentially control basal myosin oscillation and Drosophila egg chamber elongation. *Nat. Commun.* **8**, 14708. doi:10.1038/ncomms14708

Raman, R., Damle, I., Rote, R., Banerjee, S., Dingare, C. and Sonawane, M. (2016). aPKC regulates apical localization of Lgl to restrict elongation of microridges in developing zebrafish epidermis. *Nat. Commun.* **7**, 11643. doi:10.1038/ncomms11643

Russ, A., Louderbough, J. M. V., Zarnescu, D. and Schroeder, J. A. (2012). Hugl1 and Hugl2 in mammary epithelial cells: polarity, proliferation, and differentiation. *PLoS ONE* **7**, e47734. doi:10.1371/journal.pone.0047734

Schindelin, J., Arganda-Carreras, I., Frise, E., Kaynig, V., Longair, M., Pietzsch, T., Preibisch, S., Rueden, C., Saalfeld, S., Schmid, B. et al. (2012). Fiji: an open-source platform for biological-image analysis. *Nat. Methods* **9**, 676-682. doi:10.1038/nmeth.2019

Sharifkhodaei, Z., Gilbert, M. M. and Auld, V. J. (2019). Scribble and discs large mediate tricellular junction formation. *Development* **146**, dev174763. doi:10.1242/dev.174763

Sprague, B. L. and McNally, J. G. (2005). FRAP analysis of binding: proper and fitting. *Trends Cell Biol.* **15**, 84-91. doi:10.1016/j.tcb.2004.12.001

Sripathy, S., Lee, M. and Vasioukhin, V. (2011). Mammalian Llgl2 is necessary for proper branching morphogenesis during placental development. *Mol. Cell. Biol.* **31**, 2920-2933. doi:10.1128/MCB.05431-11

Stephens, R., Lim, K., Portela, M., Kvansakul, M., Humbert, P. O. and Richardson, H. E. (2018). The scribble cell polarity module in the regulation of cell signaling in tissue development and tumorigenesis. *J. Mol. Biol.* **430**, 3585-3612. doi:10.1016/j.jmb.2018.01.011

Strand, D., Jakobs, R., Merdes, G., Neumann, B., Kalmes, A., Heid, H. W., Husmann, I. and Mechler, B. M. (1994). The Drosophila lethal(2)giant larvae tumor suppressor protein forms homo-oligomers and is associated with nonmuscle myosin II heavy chain. *J. Cell Biol.* **127**, 1361-1373. doi:10.1083/jcb.127.5.1361

Tanentzapf, G. and Tepass, U. (2003). Interactions between the crumbs, lethal giant larvae and bazooka pathways in epithelial polarization. *Nat. Cell Biol.* **5**, 46-52. doi:10.1038/ncb896

Tian, A.-G. and Deng, W.-M. (2008). Lgl and its phosphorylation by aPKC regulate oocyte polarity formation in Drosophila. *Development* **135**, 463-471. doi:10.1242/dev.016253

Visco, I., Hoege, C., Hyman, A. A. and Schwille, P. (2016). In vitro reconstitution of a membrane switch mechanism for the polarity protein Lgl. *J. Mol. Biol.* **428**, 4828-4842. doi:10.1016/j.jmb.2016.10.003

Wodarz, A., Ramrath, A., Grimm, A. and Knust, E. (2000). Drosophila atypical protein kinase C associates with Bazooka and controls polarity of epithelia and neuroblasts. *J. Cell Biol.* **150**, 1361-1374. doi:10.1083/jcb.150.6.1361

Woods, D. F. and Bryant, P. J. (1989). Molecular cloning of the lethal(1)discs large-1 oncogene of Drosophila. *Dev. Biol.* **134**, 222-235. doi:10.1016/0012-1606(89)90092-4

Xu, T. and Rubin, G. M. (1993). Analysis of genetic mosaics in developing and adult Drosophila tissues. *Development* **117**, 1223-1237.

Yamamoto, S., Jaiswal, M., Charng, W.-L., Gambin, T., Karaca, E., Mirzaa, G., Wiszniewski, W., Sandoval, H., Haelterman, N. A., Xiong, B. et al. (2014). A drosophila genetic resource of mutants to study mechanisms underlying human genetic diseases. *Cell* **159**, 200-214. doi:10.1016/j.cell.2014.09.002

Yamanaka, T., Horikoshi, Y., Sugiyama, Y., Ishiyama, C., Suzuki, A., Hirose, T., Iwamatsu, A., Shinohara, A. and Ohno, S. (2003). Mammalian Lgl forms a protein complex with PAR-6 and aPKC independently of PAR-3 to regulate epithelial cell polarity. *Curr. Biol.* **13**, 734-743. doi:10.1016/S0960-9822(03)00244-6

Yamanaka, T., Horikoshi, Y., Izumi, N., Suzuki, A., Mizuno, K. and Ohno, S. (2006). Lgl mediates apical domain disassembly by suppressing the PAR-3-aPKC-PAR-6 complex to orient apical membrane polarity. *J. Cell Sci.* **119**, 2107-2118. doi:10.1242/jcs.02938

Zeitler, J., Hsu, C. P., Dionne, H. and Bilder, D. (2004). Domains controlling cell polarity and proliferation in the Drosophila tumor suppressor scribble. *J. Cell Biol.* **167**, 1137-1146. doi:10.1083/jcb.200407158

Zhu, J., Shang, Y., Wan, Q., Xia, Y., Chen, J., Du, Q. and Zhang, M. (2014). Phosphorylation-dependent interaction between tumor suppressors Dlg and Lgl. *Cell Res.* **24**, 451-463. doi:10.1038/cr.2014.16